Capability of the CALET Experiment for Measuring Elemental Abundances of Galactic Cosmic Ray Nuclei Heavier than Nickel (Z=28)

B. F. RAUCH[1], W. R. BINNS[1], M. H. ISRAEL[1], P. S. MARROCCHESI[2], Y. SHIMIZU[3], S. TORII[3,4]
[1]*Washington University, St. Louis, MO 63130, USA*
[2]*University of Siena and INFN, V. Roma 56, 53100, Italy*
[3]*Space Environment Utilization Center, JAXA, Japan*
[4]*Waseda University, 3-4-1, Okubo, Shinjuku, Tokyo 169-8555, Japan*
brauch@physics.wustl.edu
DOI: 10.7529/ICRC2011/V06/0690

Abstract: The CALorimetric Electron Telescope (CALET) is an imaging calorimeter planned for launch to the International Space Station (ISS) in 2013. The instrument consists of a segmented plastic scintillator charge measuring module, an imaging calorimeter consisting of 8 scintillating fiber planes with a total of 3 radiation lengths of tungsten plates interleaved with the fiber planes, and a total absorption calorimeter consisting of crossed lead tungstate (PWO) logs with a total of 27 radiation lengths depth. The primary objectives of the experiment are to measure electron energy spectra from 1 GeV to 20 TeV, to detect gamma-rays over the energy range from 10 GeV to 10 TeV, and to measure the energy spectra of nuclei from protons through iron. In this paper we discuss the capabilities of the instrument for measuring the abundances of nuclei heavier than nickel (Z=28). In particular we will present the maximum charge that can be detected due to instrument dynamic range, the expected charge resolution, and an estimate of the numbers of events expected in 5 years of space flight in the ISS 51.6 degree inclination orbit.

Keywords: CALET, cosmic ray, ultra-heavy

1 Introduction

As the name suggests, the CALorimetric Electron Telescope (CALET) is designed principally to measure the energy spectra of electrons, and the instrument and its principal scientific objectives are discussed in greater detail in [1, 2]. As Figure 1 shows, CALET consists, from top to bottom, of a charge detection module (CHD), an imaging calorimeter (IMC) with 3 radiation lengths of tungsten plates read out with 8 planes of scintillating fibers, and a total absorption calorimeter (TASC) with 27 radiation lengths of lead tungstate (PWO) logs. The active area of the detector decreases from 44.8 cm on a side at the CHD and IMC to 32 cm on a side in the TASC, and has a total instrument geometry factor of 0.12 m^{2}sr. The great depth of the TASC enables CALET to resolve electron energies from 1 GeV to 20 TeV, and allows the measurement of gamma-rays with energies between 10 GeV and 10 TeV. The CHD consists of two crossed layers of 3.2 cm wide $\times$ 1 cm thick $\times$ 44.8 cm long EJ204 scintillator segments, which can resolve the charges (Z) of cosmic ray nuclei with trajectory and energy corrections from the IMC and TASC [3]. CALET will thus be able to measure the energy spectra of the more abundant nuclei with $Z \leq 28$.

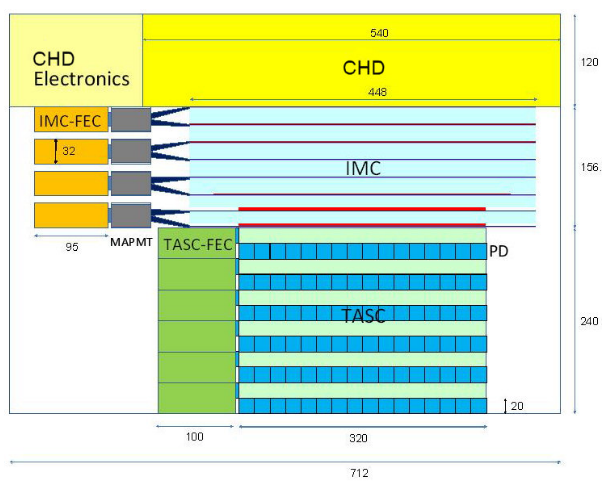

Figure 1: CALET instrument schematic side view. Dimensions are in mm.

In this paper we show that CALET can also make significant observations of the relative abundances of the ultra-heavy (UH) ($Z \geq 30$) galactic cosmic rays (GCR), the composition of which yields important clues to the source and acceleration mechanism of the GCR [4]. Previous space-based UH measurements have lacked either good charge resolution (Ariel 6 [5], High Energy Astrophysic-

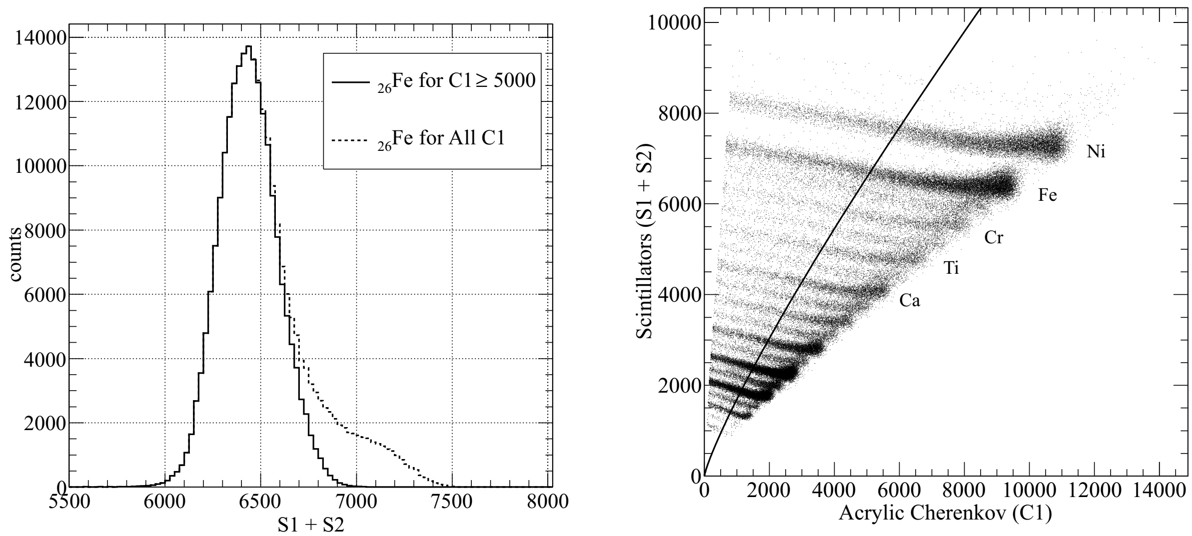

Figure 2: TIGER data from 2003 flight [4]. Left: Sum of top scintillator signals (S1 + S2) for $_{26}$Fe events for all energies (dashed line) and for acrylic Cherenkov signal C1 > 5000 ($\sim$ 600 MeV/nucleon) (solid line). Right: Scatter plot of sum of top scintillator signals (S1 + S2) versus acrylic Cherenkov signal (C1). Curve is 600 MeV/nucleon threshold.

s Observatory-3 (HEAO-3)/Heavy Nuclei Explorer (HNE) [6]), or statistics (HEAO-3-C2 [7]). The best measurements to date are from the balloon borne Trans-Iron Galactic Element Recorder (TIGER) experiment [4], and more recently with similar statistics in a complementary lower energy range with the Cosmic Ray Isotope Spectrometer (CRIS) experiment on the Advanced Composition Explorer (ACE) satellite for elemental [8] and isotopic [9] abundances. The calculations we present below show that for its anticipated five year mission CALET will have substantially improved UH statistics over previous high resolution measurements.

2 Scintillator Response to UH Nuclei

The two layers of 1 cm thick scintillator that the CALET CHD uses are similar to the two 0.8 cm thick scintillators at the top of the TIGER instrument [4]. Analysis of the CHD EJ204 scintillator shows that it has a saturated response proportional to $S \sim Z^{1.71}$ [3], while the Saint-Gobain BC-416 used in the TIGER experiment was found to have a very similar response $S \sim Z^{1.69}$ [10], so the signal dependence of the TIGER scintillators in the UH region is expected to be representative of those used in CALET. Accelerator studies of scintillator response have shown similar saturation results for nuclei up to $_{47}$Ag [11].

Examination of the dependence of the scintillator signals from the top two TIGER scintillators as a function of energy shows that the charge resolution is comparatively insensitive to energy above a certain threshold. The plot on the left in Figure 2 shows the histogram of the signal from the summed scintillators (S1 + S2) for $_{26}$Fe events for all energies (dashed histogram), and energies above an acrylic Cherenkov signal C1 > 5000 (solid histogram) corresponding to a threshold of $\sim$ 600 MeV/nucleon. The energy threshold cut yields a nearly Gaussian distribution for the charge peak. The corresponding threshold cut for 600 MeV/nucleon in the scatter plot on the right in Figure 2 shows that this cut eliminates the low energy tails from the charge contours (events to the left of the curve), which will yield resolvable peaks in the UH region as there will not be contamination from the tails of the much more abundant lower Z nuclei. The advantage is that the UH charges can be determined without the need of an energy correction and the requisite passage through the TASC.

3 Geomagnetic Rigidity Thresholds

CALET is scheduled to be installed on the International Space Station (ISS) in 2013, which has an orbit at $51.6°$ inclination, as shown in the plot on the left in Figure 3. The geomagnetic vertical cutoff rigidities at 450 km for epoch 1990 are shown in the contour plot in $15°$ longitude by $5°$ latitude bins [12], which are representative of those seen at ISS altitudes, ranging from 0 GV at the magnetic poles to over 15 GV near the equator. The dashed white curves show the rigidity threshold at 600 MeV/nucleon for $_{26}$Fe, and the exact latitude of the threshold is not very sensitive to the charge of the GCR. The plot on the right in Figure 3 shows the vertical cutoff rigidities for $_{26}$Fe as a function of orbit fraction, and it is clear that for most of its orbit aboard the ISS that CALET will be above the 600 MeV/nucleon threshold line, and only for the small fraction of the orbit

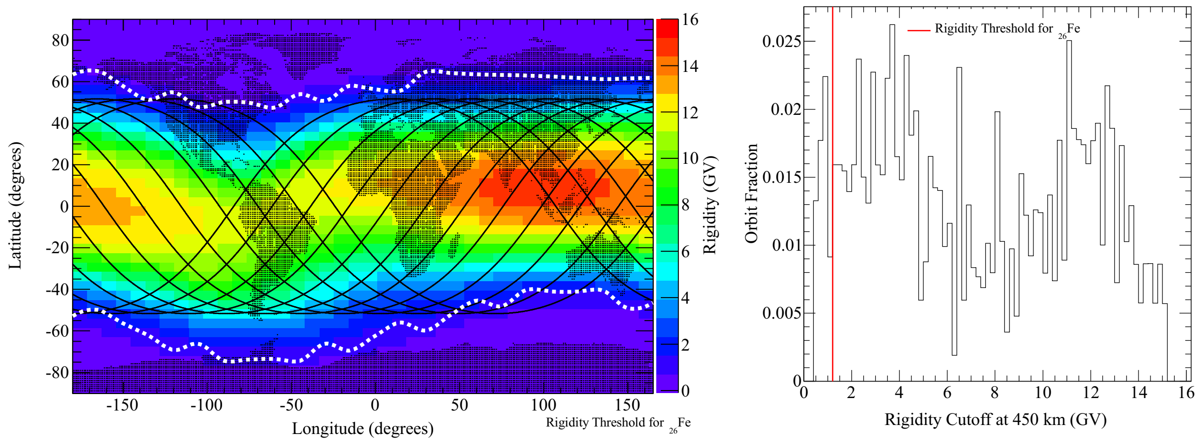

Figure 3: Left: Contour plot of geomagnetic vertical cutoff rigidities at 450 km in 15° longitude by 5° latitude bins. ISS orbit of 51.6° inclination shown in solid curves. Dashed white lines show rigidity threshold for $_{26}$Fe corresponding to 600 MeV/nucleon. Right: Histogram of vertical cutoff rigidity as a function of orbit fraction, with 600 MeV/nucleon threshold for $_{26}$Fe shown as vertical red line.

that is below the rigidity threshold will UH events require energy measurements.

4 Predicted CALET UH Measurement

Spectra have not been measured accurately for UH GCR given their extremely low fluxes, so the $_{26}$Fe spectrum scaled by relative abundances is used. Calculation of the numbers of UH events expected to be measured by CALET is a multi-step process, starting with previous measurements: HEAO-3-C2 for $Z \leq 26$ [13], TIGER for $26 \leq Z \leq 40$ [4], and HEAO-3-HNE for $Z > 40$ [6]. The derived elemental fluxes are then adjusted for screening by the magnetosphere, interaction losses within the instrument, and for CALET's response in the UH range. Expected UH measurements are then derived based on a mission duration of five years.

4.1 Energy Thresholds and Interactions

Given the anticipated launch of CALET in late 2013, the modulation it will see is likely to be between solar minimum and maximum, so calculations use averages of the results for the maximum and minimum spectra. Integral spectra are derived from the differential spectra in [14], and the elemental abundances are calculated for each latitude and longitude bin by evaluating the integral spectra at the appropriate rigidity threshold energy. The contribution from each bin is then weighted by total residence time for the projected five year mission, and then reduced by the fraction of events that would interact due to the amount of material traversed as a function of the differential geometry using total charge changing cross sections [15].

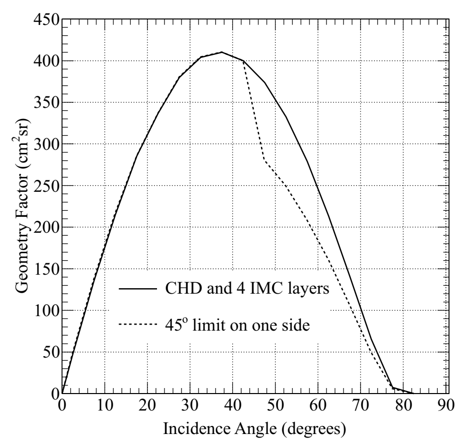

Figure 4: Differential geometry factor for CALET CHD and top 4 IMC layers (solid line), and with 45° limit on one side (dashed line).

4.2 Differential Geometry Factor

As noted above, at high enough energies the charges of UH GCR can be determined based on trajectory corrected scintillator signals without an energy correction, and this only requires passage through the CHD and the top four layers (five fiber planes) in the IMC, but not the TASC. This gives a larger total geometry factor, 0.40 m^{2}sr, than for the total instrument, 0.12 m^{2}sr, which significantly increases the statistics of the UH measurement. There is a further constraint that one side of the CALET instrument cannot view particles with trajectories beyond 45° due to occlusion by structural material. The differential geometry factor used in this calculation is shown in Figure 4 as the dashed line.

4.3 Dynamic Range

The final step in determining the numbers of events that CALET will see is to account for the limits imposed by the instrument's dynamic range. The signal processing chain in the CHD represents the limiting factor in the dynamic range, with the limits of the photomultiplier tubes (PMT), charge sensitive amplifiers (CSA), and analog to digital converters (ADC) each contributing to the dynamic range, as shown in Figure 5. Considering the scintillation signal expected at $45°$ incidence the limiting factor in the chain appears to be the ADC with an upper limit of a resolved charge of $Z \sim 46$.

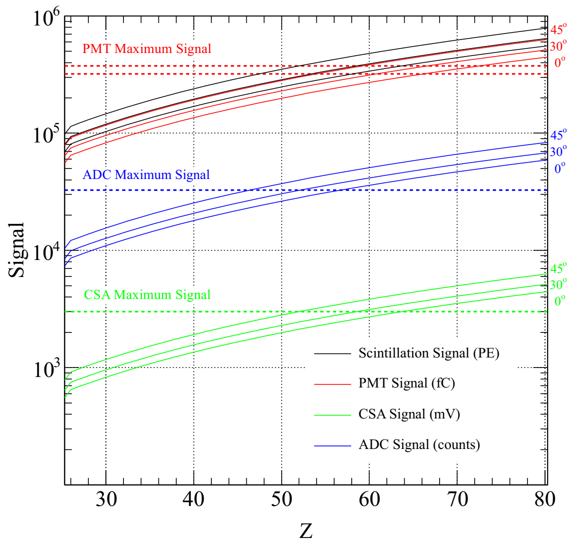

Figure 5: Charge dependence in CALET signal processing chain with dynamic range limits.

5 Conclusions

Figure 6 shows the predicted numbers of UH events for CALET (histogram) and the numbers of events of the combined TIGER dataset (points) [4]. In the $30 \le Z \le 40$ charge range of the UH GCR CALET should obtain numbers of events $\sim 5\times$ that of TIGER, which is similar to the numbers of events expected from Super-TIGER for 60 days at float [16]. The advantage of CALET is that the measurements will be made above the atmosphere, so there will be smaller corrections for nuclear interactions. In the $40 \le Z \le 46$ charge range CALET can make exploratory measurements with statistical precision of $\sim 25 - 30\%$ for even-Z nuclei to the highest charge resolved by the dynamic range of the instrument.

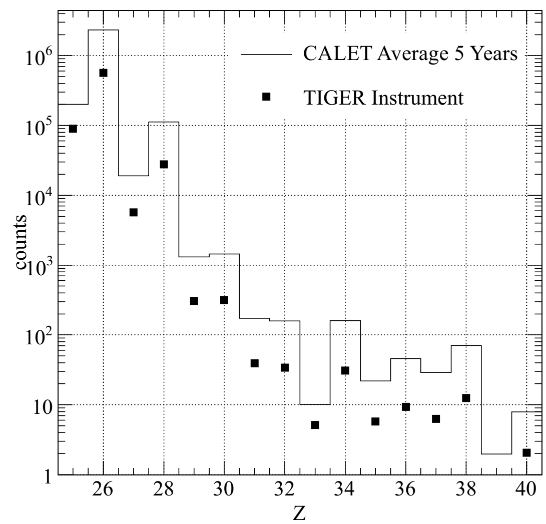

Figure 6: Comparison of anticipated CALET UH numbers of events compared with TIGER data [4].

6 Acknowledgments

This research was supported by NASA at Washington University under Grant Number NNX11AE02G.

References

[1] S. Torii for the CALET Collaboration, Proc. 32nd ICRC, 2011, ID 615
[2] K. Yoshida for the CALET Collaboration, Proc. 32nd ICRC, 2011, ID 766
[3] Y. Shimizu, et al., Proc. 32nd ICRC, 2011, ID 898
[4] B. F. Rauch, et al., ApJ, 2009, **697**: 2083-2088
[5] P. H. Fowler, et al., ApJ, 1987, **314**: 739-746
[6] W. R. Binns, et al., ApJ, 1989, **346**: 997-1009
[7] B. Byrnak, et al., Proc. 18th Int. Cosmic Ray Conf., 1983, **2**: 29-32
[8] M. H. Israel, et al., Proc. 32nd ICRC, 2011, ID 657
[9] W. R. Binns, et al., Proc. 32nd ICRC, 2011, ID 649
[10] B. F. Rauch: 2008, Ph.D. thesis, Washington University, St. Louis
[11] W. R. Binns, et al., Proc. 22nd ICRC, 1991, **2**: 511-514
[12] D. F. Smart and M. A. Shea, AdSpR, 2009, **44**: 1107-1123
[13] J. J. Engelmann, et al., A&A, 1990, **233**: 96-111
[14] J. S. George, et al., ApJ, 2009, **698**: 1666-1681
[15] B. S. Nilsen, et al., PhRvC, 1995, **52**: 3277-3290
[16] J. W. Mitchell, et al., Proc. 32nd ICRC, 2011, ID 1234